Soil N_2O emission potential falls along a denitrification phenotype gradient linked to differences in microbiome, rainfall and carbon availability

Matthew P. Highton[1], Lars R. Bakken[2], Peter Dörsch[3], Steve Wakelin[4, 5], Cecile A. M. de Klein[6], Lars Molstad[3], Sergio E. Morales[1,*]

Highlights

- N_2O emission potential is linked to microbiome changes associated with rainfall, but not to pH.
- Sequential vs. concurrent denitrification phenotypes differing in NO and N_2O accumulation are identified.
- High N_2O accumulation is associated with increased NO accumulation.
- Sequentiality of N_2O production/reduction determines soil N_2O emission potential.
- Sequentiality of N_2O reduction was susceptible to manipulation via carbon addition.

Soil N_2O emission potential falls along a denitrification phenotype gradient linked to differences in microbiome, rainfall and carbon availability

Matthew P. Highton[1], Lars R. Bakken[2], Peter Dörsch[3], Steve Wakelin[4, 5], Cecile A. M. de Klein[6], Lars Molstad[3], Sergio E. Morales[1,*]

[1]Department of Microbiology and Immunology, University of Otago, Dunedin, New Zealand

[2]Faculty of Chemistry, Biotechnology and Food Science, Norwegian University of Life Sciences, Ås, Norway

[3]Faculty of Environmental Sciences and Natural Resource Management, Norwegian University of Life Sciences, Ås, Norway

[4]AgResearch Lincoln Science Centre, Christchurch, New Zealand

[5]Scion Research, Christchurch, New Zealand

[6]AgResearch Invermay, Mosgiel, New Zealand

*Corresponding Author

Keywords: Denitrification phenotype, N_2O emission potential, microbiome, rainfall, carbon availability, *nosZ*

Abstract

Soil denitrification produces the potent greenhouse gas nitrous oxide (N_2O) and by further reduction of N_2O, the harmless inert gas N_2. N_2O emission is determined by rate and timing of the N_2O producing and reducing steps which are sensitive to a series of proximal and distal regulators such as pH and microbial community composition. Microbial community associations to N_2O emission potential ($N_2O/(N_2O+N_2)$) are commonly entangled with pH leaving the true role of community composition unclear. Here, we leverage a set of soil microbiomes strongly linked to rainfall above pH to test the hypothesis that microbiome vs. N_2O emission potential ($N_2O/(N_2O+N_2)$) correlations will be maintained across alternative distal drivers. N_2O emission potential ($N_2O/(N_2O+N_2)$) and denitrification gas (NO, N_2O, N_2) kinetics were assessed by automated gas chromatography while community composition was assessed by 16S rRNA gene sequencing and qPCR of *nosZI* and *II* genes. Analyses revealed a sustained correlation between microbiome and N_2O emission potential ($N_2O/(N_2O+N_2)$) in the absence of a pH effect. Further, a continuum of gas accumulation phenotypes linked to NO accumulation and sensitive to carbon addition are identified. Separate phenotypes carried out N_2O production and reduction steps more concurrently or sequentially and thus determined N_2O accumulation and emission potential ($N_2O/(N_2O+N_2)$). Concurrent N_2O producing/reducing soils typically contained NO accumulation to a low steady state, while carbon addition manipulations which increased NO accumulation also increased sequentiality of N_2O production/reduction and thus emission potential ($N_2O/(N_2O+N_2)$). These features may indicate a conserved NO inhibitory mechanism across multiple effectors (rainfall, community composition, carbon availability).

Introduction

Production and emission of nitrous oxide (N_2O) represents a significant climate concern due to its high global warming potential (298 times that of CO_2 over a 100 year time span on a mass to mass basis) (Myhre *et al.*, 2013) and ozone depleting activity (Ravishankara *et al.*, 2009). The most recent IPCC report ranks N_2O as the third most significant greenhouse gas, accounting for 6.2% of global climate forcing (Intergovernmental Panel on Climate Change, 2013). Atmospheric concentrations of N_2O have risen dramatically over the past century to a current concentration of greater than 333 ppb (Jan, 2020; 2° Institute, 2016), much of which is attributed to anthropogenic soil emissions (Davidson, 2009). Global N_2O budgets suggest that around 45% of the emitted N_2O is produced anthropogenically with the majority (60%) coming from agricultural sources (Syakila and Kroeze, 2011). In an agricultural setting, N_2O production is traditionally attributed to denitrification and nitrification (Bremner, 1997) of N in animal excreta or applied fertilizers (Davidson, 2009; Syakila and Kroeze, 2011; Oenema *et al.*, 2005) but a number of other biological processes are also relevant (Baggs, 2011).

Denitrification occurs under anoxic conditions when microbial populations switch from O_2 based respiration to reduction of nitrogenous molecules ($NO_3^- \rightarrow NO_2^- \rightarrow NO \rightarrow N_2O \rightarrow N_2$). In each step, reduction of the nitrogenous molecule as a terminal electron acceptor is catalyzed by an independent reductase enzyme (nitrate reductase-Nar or Nap, nitrite reductase-Nir, nitric oxide reductase-Nor, and nitrous oxide reductase-Nos) (Zumft, 1997). The last step in the process, N_2O reduction, is an important focus in denitrification and greenhouse gas research (Jones *et al.*, 2014; Liu *et al.*, 2014; Richardson *et al.*, 2009) as it determines whether the final gaseous product of denitrification is the greenhouse gas N_2O or the harmless inert gas N_2. In fact, N_2O reductase is the only known biological sink of N_2O (Thomson *et al.*, 2012), therefore, encouraging complete denitrification at the time

of N_2O production represents an important strategy to preventing further rise in atmospheric concentrations (Richardson *et al.*, 2009). In reality, N_2O vs. N_2 production is not binary (only N_2O or N_2 produced) and N_2O to N_2 product ratios depend on a great number of factors including pH (Simek and Cooper, 2002), carbon and nitrate (NO_3^-) availability (Senbayram *et al.*, 2012), as well as nitrite (NO_2^-) (Firestone *et al.*, 1979; Gaskell *et al.*, 1981).

Conceptually, factors affecting N_2O emission ratios can be separated into i) microbial community genetic potential for each denitrification step, ii) distal factors, determining that genetic potential in the long term, and iii) proximal factors, acting within genetic potential on short term time scales to impact instantaneous denitrification rates (e.g. carbon and NO_3^- concentrations), (Wallenstein *et al.*, 2006; Groffman *et al.*, 1988). There has been some debate over the relative importance of these factors and disentangling their effects can be difficult when factors such as pH have both immediate effects on enzymatic activity during denitrification and distal effects on denitrification potential (Samad *et al.*, 2016b).

The effect of pH on soil N_2O emissions is well documented (Simek and Cooper, 2002). Low soil pH results in higher soil $N_2O/(N_2O+N_2)$ ratios, most clearly demonstrated in pH manipulations of soils from the same site (Čuhel *et al.*, 2010; Liu *et al.*, 2010; Simek and Cooper, 2002), but also manifests in differences in N_2O product ratios between sites (Samad *et al.*, 2016b). Bergaust *et al.* (2010) showed evidence for a post-transcriptional effect on the formation of functional N_2O reductase at low pH in pure culture experiments, possibly due to impeded assembly of this periplasmic enzyme at low pH. A similar post transcriptional phenomenon was supported using microbial consortia extracted from soils with different native pH (Liu *et al.*, 2014). Contrastingly, some studies have demonstrated that pH effects on N_2O reduction are dependent on the concentration of NO_3^- or NO_2^- (Blackmer and Bremner, 1978; Firestone *et al.*, 1979; Gaskell *et al.*, 1981). Blackmer and

Bremner (1978) showed that pH had negligible effects on N_2O reduction activity of soils in the absence of supplied NO_3^- while other studies observed and increased inhibitory impact of NO_3^- or NO_2^- under decreasing pH (Firestone *et al.*, 1979; Gaskell *et al.*, 1981). To confuse matters further, pH probably also has long term distal effects on denitrification potential due to its well-known impact on microbial community structuring (Lauber *et al.*, 2008; Kaminsky *et al.*, 2017) and probably more specifically the abundance and ratios of denitrification genes (e.g. Samad *et al.*, 2016b; Domeignoz-Horta *et al.*, 2015; Jones *et al.*, 2014).

The functional and taxonomic composition of denitrifier communities has become an important focus of denitrification research due to advances in molecular tools. Denitrifying microbes may carry all or only some of the full denitrification gene repertoire and therefore changes in the phylogenetic composition of denitrifier communities can affect the ratio of genes coding for N_2O reductase to those coding for N_2O producing enzymes, thus determining the genetic potential for N_2O emission (Graf *et al.*, 2014; Roco *et al.*, 2017). Graf *et al.* (2014) showed that the organisms carrying the *nosZII* gene encoding nitrous oxide reductase clade II commonly had a truncated denitrification pathway without the genes encoding the preceding denitrification steps. Implicit to this finding is the suggestion they may reduce $N_2O/(N_2O+N_2)$ ratios by acting as N_2O sinks. Jones *et al.* (2014) showed evidence for N_2O sink capacity related to low *nosZI/nosZII* ratios, though controversial because the results could also be explained as a direct (proximal) effect of soil pH (Bakken *et al.*, 2015). $N_2O/(N_2O+N_2)$ product ratios have been linked to differences in overall microbial community structure as measured by 16S rRNA gene sequencing, suggesting that this could be used as a predictor of N_2O emission potential (Morales *et al.*, 2014; Samad *et al.*, 2016b). However, it remains unclear whether these correlations indicate a true causal relationship. For example Samad *et al.* (2016b) linked 16S community composition to soil $N_2O/(N_2O+N_2)$ product ratios but both these measures were also correlated to soil pH.

Therefore, the results are possibly explained by the well documented but separate effects of pH on $N_2O/(N_2O+N_2)$ (Simek and Cooper, 2002) and on microbial community composition (Lauber *et al.*, 2009; Kaminsky *et al.*, 2017).

N_2O accumulation during denitrification may also be caused by differential flow of electrons to the separate N-reductases (Pan *et al.*, 2013). In wastewater treatment, low carbon (reductant) availability enhances competition for electrons between N_2O and upstream N-reductases which can result in transient N_2O accumulation (Pan *et al.*, 2013; Ribera-Guardia *et al.*, 2014). Indeed carbon and substrate availability can affect $N_2O/(N_2O+N_2)$ product ratios in many contexts including soils, though the direction of the effect is not always consistent (Gillam *et al.*, 2008; Senbayram *et al.*, 2012; Weier *et al.*, 1993).

Here, we aimed to re-assess the consistency of previously outlined (Samad *et al.*, 2016b, 2016a) linkages between $N_2O/(N_2O+N_2)$, microbial community composition (as measured by 16S rRNA gene sequencing and qPCR of *nosZ* genes) and pH in a larger alternative cohort (20 soils) of pasture soils. Previous investigations indicated community composition in the present soil set was correlated to changes in long term rainfall above pH and we hypothesized microbiome to N_2O emission potential associations would be maintained across this alternate distal driver. Anoxic soil incubations revealed contrasting $N_2O/(N_2O+N_2)$ and denitrification phenotypes based on the timing of N_2O reduction which determined the propensity for soil N_2O emission. We further assessed the phenotypes and $N_2O/(N_2O+N_2)$ ratios in relation to potential proximal controls (NO_3^- + NO_2^- concentration, carbon availability) based on 2 alternate hypotheses: 1) N_2O reduction activity was impaired by higher NO_3^- + NO_2^- concentrations. 2) Impaired N_2O reduction in high $N_2O/(N_2O+N_2)$ ratio soils is caused by limited carbon availability and thus electron supply to N_2O reductase.

Materials and methods

2.1 Soil collection

Soils were sampled at 20 sites representing sheep, dairy, beef and goat farms across multiple regions of New Zealand's South Island. Sampling begun on the 2nd of September 2016 and continued through until the 8th of September. At each site, soil cores (10 cm depth, 2.5 cm diameter) were sampled at 2.5 m intervals across a 7.5 m transect (0 m, 2.5 m, 5 m, 7.5 m) using a stainless steel auger. Triplicate cores were collected for each distance and composited in a bag (12 pooled cores) while a fourth core from each distance was kept separate for molecular analyses (4 cores). If topsoil was less than 10cm deep, additional cores were taken to make up the volume. Soil cores were stored in partially open ziplock bags (to prevent anoxia) on ice until sampling was completed. Pooled cores were homogenized, and worms, insects, grass and large roots removed before field moist storage at 4ºC. Core samples for molecular analysis were immediately frozen at -80ºC until DNA extraction. See Table S1 for basic soil descriptors based on current analyses and data collected from separate sampling in 2011 (Wakelin *et al.*, 2013).

Pooled site cores were transported to the Norwegian University of Life Sciences (NMBU, Ås, Akershus, Norway), where they were sieved (2mm) and stored at 4ºC before initiating kinetic experiments.

2.2 Nitrate + nitrite measurements

Endogenous soil nitrate + nitrite (NO_3^- + NO_2^-) content was measured in sieved pooled soils using 0.2g of each soil with 1mL of 2M KCl extractant in 1.5 mL microfuge tubes (Lim *et al.*, 2018). Slurries were shaken and spun down at 16000G for 2 minutes before recovering the supernatant into fresh 1.5mL microfuge tubes. NO_3^- + NO_2^- concentration was quantified by chemical reduction to nitric oxide (NO) followed by

chemiluminescent detection as detailed by (Braman and Hendrix, 1989;Lim *et al.*, 2018). In brief, 10µL of supernatant was introduced into a sealed glass piping system containing a heated (95ºC) acid vanadium chloride solution (50mM VCl_3 in 1M HCl). VCl_3 reacts to reduce NO_3^- quantitatively to NO_2^- before converting it to NO gas. The NO gas was captured and carried in an N_2 stream to a Sievers Nitric Oxide Analyzer 280i system (GE Analytical Instruments, Boulder, CO, USA) for quantification. Standard KNO_3 solutions (100 to 0.01mM) were used to calibrate the area under detection signal peaks allowing calculation of NO_2^-+NO_3^- concentration in soil supernatants. NO_2^-+NO_3^- per gram soil or per µL porewater was back calculated based on KCl dilution factor, and soil dry weight/moisture weight (as determined gravimetrically below) .

2.3 Nitrate adjustment

Soil moisture was determined gravimetrically by drying 5-10g soil at 60ºC for minimum 24h (ASTM D2216-10, 2010). Prior to incubation, soils were supplemented with NO_3^- and ammonium by flooding and draining with a 2mM NH_4NO_3 solution e.g. (Samad *et al.*, 2016a; Liu *et al.*, 2010; Qu *et al.*, 2014). NO_3^- supplied N for denitrification while ammonium acted as a preferential assimilatory N source. For this, an 80g dry weight equivalent of soil was placed in a 500mL Sterafil Filter Holder (Merck, Burlington, MA, USA) and flooded with 300mL of 2mM NH_4NO_3 (sufficient volume to dilute endogenous NO_3^-) . After 15min the solution was drained through a 0.2µM cellulose filter (Merck) with 1.2µM glass-fibre pre filter (Merck) using a vacuum manifold. Soils were mixed and a subsample was taken for overnight moisture content analysis (5g, as above). The remainder of the soils was stored overnight in funnels covered with aluminum foil before use in incubation experiments the next day.

2.4 Gas kinetics measurements

Respiration and denitrification activity of soils was measured by gas chromatography of headspace gases (O_2, CO_2, NO, N_2O, N_2) in oxic and anoxic batch incubations commencing between 39 and 56 days post sampling. The temperature controlled robotic autosampler, gas chromatograph (Agilent GC -7890A equipped with ECD, TCD, FID) and chemiluminescence NOx analyzer (Model 200A, Advanced Pollution Instrumentation, San Diego, USA) used here are described in detail by (Molstad *et al.*, 2007; Qu *et al.*, 2014). The device holds up to 44 sealed 120 mL serum vials in a temperature controlled water bath. A robotic arm equipped with a hypodermic needle and a peristaltic pump takes headspace gas samples periodically and pumps them through dedicated sample loops in the GC. The GC uses helium as carrier gas while subsequent back pumping replaces sampled gas with helium thus maintaining the pressure in the serum vials at ~1 atm. Dilution and leakage are back calculated following experiment completion to allow estimation of true gas production. Here, 20g dry weight equivalent of NH_4NO_3 adjusted soil was placed in triplicate 120mL serum vials and crimp sealed with butyl rubber septa. A 15g subsample of each soil was frozen at the start of each incubation for subsequent measurement of NO_2^- +NO_3^- concentrations as described above. The serum vials were placed in the water bath (20ºC) under the autosampler and allowed to equilibrate before releasing overpressure through a water filled syringe without piston. Additional vials (duplicates) were filled with premixed standard gases (including 400ppm CO_2, 10,000ppm CO_2, 500ppb N_2O, 151ppm N_2O, 25ppm NO) supplied by AGA industrial gases (Oslo, Akershus, Norway), compressed air (781,000ppm N_2, 200900ppm O_2) or helium. The autosampler was programmed to take headspace samples every ~5hrs. After 7 rounds of sampling, at ~40hrs, anoxia was induced by helium flushing the vials (3 cycles of evacuation for 180sec and He-filling for 20sec) and incubation was continued until most soils had converted all denitrification products to N_2. Two separate experiments were required 10 days apart to process all 20 soils.

2.5 Measures of N_2O emission potential/kinetics

The N_2O hypothetically emitted (%) metric was calculated as max µmol N_2O-N accumulated in vial expressed as a percentage of final cumulative N (N_2-N). N_2O hypothetically emitted (%) was used to evaluate the sequentiality of N_2O production and reduction steps over the course of an incubation and the relative N_2O emission potential of each soil. It is equivalent to typical N_2O product ratios ($N_2O/N_2O + N_2$) but expressed relative to total final accumulated N rather than just gaseous N_2O+N_2 at the timepoint of calculation. It is our preferred metric because:

1) It is event based (i.e. calculated at peak in vial N_2O). This allows comparison of soils with divergent denitrification timescales/rates.

2) It is a relative measure (i.e. expressed as a percentage of total N finally accumulated). This allows comparison of soils with contrasting initial NO_3^- supply and net denitrification rates.

3) It describes N_2O emission potential (i.e. soils accumulating greater peak N_2O in headspace are likely to be higher emitters in situ). This N_2O is likely to be emitted in an unsealed environment therefore this metric ignores net N_2O reconsumption from the headspace.

4) It directly describes the sequentiality of N_2O production/reduction (i.e. to what degree N_2O production and reduction to N_2 were carried out at the same time and to the same magnitude, thus mitigating N_2O accumulation). This was highly relevant to the soil kinetics observed here (see results).

Additional emission potential metrics were evaluated to allow comparison with previous studies. $N_2O/(N_2O+N_2)$ (N_2O ratio) calculated as µmol cumulative N_2O-N (per vial) over max µmol cumulative N_2O-N plus µmol cumulative N_2-N at various timepoints

239 ($N_2O/(N_2O+N_2)$ (max N_2O), $N_2O/(N_2O+N_2)$ (50hrs)) (Samad *et al.*, 2016a). N_2O index
240 (I_{N2O}) as used previously (Liu *et al.*, 2010; Qu *et al.*, 2014; Samad *et al.*, 2016a), calculated
241 as the area under a N_2O curve over the area under an N_2O curve + N_2 curve using the
242 following formula: $I_{N_2O} = \int_0^T N_2O(t)dt \; / \; \int_0^T [N2O(t) + N_2(t)]dt$

243 It is useful because it allows a time-integrated view of N_2O vs. N_2 stoichiometry. Areas are
244 calculated for each time period between two sampling points (~5hrs) and summed up to an
245 arbitrary time point (T). Here, we used 50hrs (I_{N2O} (50hrs)) and once all denitrification gas
246 was accumulated as N_2 (I_{N2O} (N_2 plateau)).

247 N_2O hypothetically emitted (%) value cut-offs were assigned to separate N-gas
248 accumulation patterns into discrete phenotypes based on N_2O, NO, and N_2 accumulation
249 patterns. Sequential soils (88% to 100%) had close to 0 accumulation of N_2 before peak
250 N_2O, a sudden increase in N_2 rate was observed after peak N_2O, and a single often high NO
251 peak was usually observed. Concurrent soils (0 to 80%) developed N_2 production early
252 which was either sustained or gradually increased. NO levels were typically controlled
253 after a brief peak. Intermediate soils (81% to 87%) had features of both phenotypes. NO
254 was typically poorly controlled, some N_2 production was observed before peak N2O but
255 sharp increases in N_2 rate were observed after peak N_2O.

256 **2.6 pH measurement**

257 For each soil, a 10mL subsample was placed in a plastic container using a volumetric
258 spoon and 20mL of 10mM $CaCl_2$ was added. Containers were capped and shaken until the
259 soil was dispersed in the solution. Soils were left overnight at room temperature. Soils were
260 re-dispersed by shaking and left to settle for 10min before the pH was measured in the
261 supernatant using a H170 pH meter (Hach, Loveland, CO, USA).

262 **2.7 Rainfall**

Average daily rainfall at the sample sites (mm day^{-1}) was estimated at various timescales (month, year, 10 years) using rainfall data from New Zealand's national climate database. Data were assessed through the CliFlo web system (NIWA, 2017). Collected data spanned from 08/09/96 to 07/09/2016. We also included rainfall and potential evapotranspiration estimates from a previous study (Wakelin *et al.*, 2013) on the same soils (rainfall historical) which used average daily measurements for 5 years prior to sampling. Values were calculated through interpolations (Cichota *et al.*, 2008; Tait *et al.*, 2005) using the Virtual Climate Station from NIWA (Wellington, Wellington, New Zealand). Drainage class (1: very poor to 5: well) was collected from the New Zealand Fundamental soil Layer (LRIS, 2020).

2.8 DNA extraction

Distance-specific site cores (0m, 2.5m, 5m, 7.5m) were defrosted for DNA extraction. To test if pooling and sieving was necessary for future sampling, a subsample of 15g fresh weight from each core was pooled into a mixed sample (mixed-m) and a subsample of this sample was sieved through a 2mm sieve (mixed and sieved-ms). ~0.25g of each distance specific sample per site and the two additional m and ms samples per site (6 samples per site times 20 sites = 120 samples) were extracted using a Powersoil DNA Isolation kit (Mobio, Carlsbad, CA, USA) according to the standard instructions. Bead beating was carried out at 1500rpm in two 15sec steps with intermittent cooling using a 1600 MiniG cell-lyser (SPEXSamplePrep, Metuchen, NJ, USA). DNA extracts were quantified and quality checked using a Qubit fluorometer (Invitrogen, Carlsbad, CA, USA) with Qubit dsDNA HS assay (Invitrogen) and NanoDrop One (Thermo Scientific, Waltham, Massachusetts, USA). pH-$CaCl_2$ and pH-H_2O of ms soils was measured as described earlier (section 2.2.2, pH measurement) but using a MP22O pH meter with Inlab 413 electrode (Mettler Toledo, Columbus, Ohio, USA).

2.9 16S amplicon sequencing

16S amplicon sequencing was carried out on a single lane of an Illumina HiSeq using Version 4_13 of the Earth Microbiome Project standard protocol (Caporaso *et al.*, 2012). Open reference OTU picking (97% similarity, UCLUST (Edgar, 2010) and taxonomy assignment (BLAST (Altschul *et al.*, 1990) was carried out in QIIME 1.9.1 (Caporaso *et al.*, 2010) using version 128 of the SILVA database (Quast *et al.*, 2013). Site-specific sequence pools were then subsampled 10 times to a depth of 37120 sequences. Subsampled pools were averaged using basic R functions (R Core Team, 2016). NMDS ordinations (Bray Curtis dissimilarity) were carried out using Phyloseq (McMurdie and Holmes, 2013). Mantel tests were carried out in Vegan (Dixon, 2003) using a Pearson correlation method. Sequences have been submitted to the NCBI Sequence Read Archive under accession numbers SRR11650167 to SRR11650286 and BioProject ID PRJNA629050.

2.10 qPCR

Total prokaryotic abundance, and nitrous oxide reductase gene abundance for Clade I and II were measured by targeting the 16S rRNA gene and *nosZ* gene respectively, using the following primer pairs: 16S UNIV F&R (Hartman *et al.*, 2009), nosZ2F & nosZ2R (Henry *et al.*, 2006) , 1153_nosZ8F & 1888_nosZ29R (Jones *et al.*, 2013). Reactions (10µL total volume) consisted of 10ng soil DNA, forward and reverse primers at a final concentration of 0.5µM (except for *nosZ II* reactions which included 1µM), 5µL of Luminaris HiGreen low Rox qPCR Master Mix (Thermo Scientific) and nuclease free water (Thermo Scientific) to make up the 10µL volume. Minimum triplicate reactions per sample were performed using a QuantStudio 6 flex qPCR machine (Applied Biosystems, Foster City, CA, USA) according to the following thermal cycling conditions. 16S: 2 min UDG pre-treatment at 50ºC, 10min initial denaturation at 95ºC, 40 cycles of 15sec denaturation at 95ºC, 30sec annealing at 65ºC and 30sec extension at 72ºC. *nosZI*: 2 min

313 UDG pre-treatment at 50ºC, 10min initial denaturation at 95ºC, 40 cycles of 15sec
314 denaturation at 95ºC, 30sec annealing at 58.5ºC and 30sec extension at 72ºC. *nosZII*
315 touchdown: 2 min UDG pre-treatment at 50ºC, 10min initial denaturation at 95ºC, 6 cycles
316 of amplification decreasing annealing temperature by 1ºC per cycle consisting of 15sec
317 denaturation at 95ºC, 30sec annealing at 60-55ºC and 30sec extension at 72ºC, 44 cycles of
318 amplification consisting of 15sec denaturation at 95ºC, 30sec annealing at 54ºC, 30sec
319 extension at 72ºC and 30sec at 80ºC for signal detection. All reaction plates included
320 minimum triplicate no-template controls and a 10-fold dilution series of pGEM-t-easy
321 (Promega, Madison, WI, USA) cloned standards for the relevant amplicon, encompassing
322 the sample quantification range. Measurement of the desired amplicon was confirmed by a
323 melt curve analyses (15sec denaturation at 95ºC, 1min 60ºC, 30 sec 95ºC) following target
324 amplification.

325 **2.11 Predicted NO_3^- + NO_2^- accumulation and predicted nitrification**

326 Predicted NO_3^- + NO_2^- at the start of anoxia was calculated as the final accumulated
327 µmol-N accumulated in each vial at the end of the incubation. Predicted nitrification during
328 the oxic period was calculated as the difference between measured NO_3^- + NO_2^- at the
329 beginning of the experiment and predicted NO_3^- + NO_2^- at the start of anoxia.

330 **2.12 Carbon amendment experiment**

331 An independent experiment was set up as described above with some modifications
332 to test the influence of carbon availability on gas kinetics. Incubations commenced 3
333 months after initial sampling. Five soils were selected based on covering a range of N_2O
334 ratios (40-Fairlie Geraldine, 20-Waitaha, 1-Woodend, 33-Rae's Junction, 5-Waipapa). In
335 these incubations, an initial period of oxic storage and incubation was not carried out and
336 the concentration of NH_4NO_3 in flooding solutions was increased (4mM) to account for
337 extra NO_3^- accumulated during the oxic period in the original incubations. Incubations were

monitored under two treatment conditions: 4mM NH_4NO_3, ± 10mM sodium glutamate as a carbon source. Glutamate can be utilised by most bacteria and in addition could provide a preferential organic N source preventing NO_3^- assimilation (Halvorson, 1972). Sodium glutamate solutions were pH adjusted to the soils' native pH using HCl.

2.13 Statistical analyses

Incubation kinetics variables are presented and used in correlations as the mean of triplicate incubations or duplicate incubations in cases where a replicate had to be dropped due to gas leakage. Spearman's ranked correlations between incubation kinetic measures and soil variables were used based on non-normaly distributed data. Discrete phenotypic groups were compared to incubation variables using a Wilcoxon rank sum test (differences of medians) with chi-squared approximation (but are also supported with continuous/ranked analyses). NMDS plots were evaluated based on stress <0.2. NMDS plots are presented for a single pooled sample per soil for appropriate statistical comparison to gas kinetic and environmental variables but ordinations with full distance specific replicates are available (Figure S3). Bray Curtis dissimilarity matrixes were compared against incubation and environmental variables by Mantel test using a pearson correlation co-efficient.. NMDS axis 1 and 2 co-ordinates were also extracted and tested against incubation and environmental variables using a spearman's ranked correlation to identify variables associated with a particular axis. Multiple linear regression for prediction of N_2O hypothetically emitted (%) using rainfall, soil drainage class and potential evapotranspiration was performed using standard least squares.

359 **Results**

360 **3.1 Denitrification gas kinetics**

361 We monitored gas production (CO_2, NO, N_2O, N_2) from NH_4NO_3 amended soil
362 incubations to identify soils with contrasting denitrification gas production kinetics and
363 potential for N_2O emission (key incubation variables available in Table S2). Soils were
364 initially incubated under oxic conditions (40hrs) to identify their aerobic respiratory
365 potential. Soil CO_2 production was in the range of 1 to 5μmol hr^{-1} $vial^{-1}$ (mean ± SD = 3.43
366 ± 2.89) with the exception of one soil (18-Kumara, a flipped pasture) that had a production
367 rate of 15.21μmol hr^{-1} $vial^{-1}$.

368 During the subsequent anoxic incubation period, soils varied greatly in the timing of
369 N_2O production and further reduction to N_2: while some soils carried out concurrent N_2O
370 production/reduction from the onset of anoxia, others carried out each step sequentially,
371 accumulating most N as N_2O before converting it stoichiometrically to N_2 (Figure 1). We
372 evaluated the sequentiality of N_2O production/reduction on a continuous scale using N_2O
373 hypothetically emitted (%) and applied somewhat arbitrary cutoffs (see section 2.5.) to
374 place each soil in discrete phenotypic groups: concurrent (0 to 80%), intermediate (81% to
375 87%) and sequential (88% to 100%). In addition to timing of N_2O production/reduction,
376 alternative phenotypic groups had contrasting NO accumulation patterns: more concurrent
377 N_2O producing/reducing soils accumulated far less NO (Spearman's correlation, average
378 μmol NO $vial^{-1}$ vs. N_2O hypothetically emitted %, $\rho=0.80$, $p<0.0001$), and most displayed a
379 very low pseudo steady state NO level after a brief peak in accumulation (Figure 1A).

380 N_2O hypothetically emitted (%) was also used to evaluate soil N_2O emission potential
381 as sequentiality of N_2O production/reduction determines N_2O accumulation, while omitting
382 the reconsumption of headspace N_2O predominant late in sequential soils which is more

likely to be emitted in an unsealed environment. Alternative measures of N_2O emission potential were also evaluated to maintain comparability with previous studies and gave similar soil rankings (Spearmans correlation vs. N_2O hypothetically emitted %, $N_2O/(N_2O+N_2)$ (max N_2O): $\rho=0.94$, $p<0.0001$, $N_2O/(N_2O+N_2)$ (50hrs): $\rho=0.71$, $p<0.001$, I_{N2O} (N_2 plateau): $\rho=0.79$, $p<0.0001$, I_{N2O} (50hrs): $\rho=0.53$, $p<0.05$).

3.2 Interaction between N_2O emission potential, pH and community composition

We hypothesized that the observed kinetic patterns/N_2O emission potentials were linked to differences in pH and community differences based on previously observed linkages between N_2O product ratios, pH and 16S microbial community composition using the same incubation methodology (Samad *et al.*, 2016b). N_2O hypothetically emitted (%) was not correlated with soil pH (Spearman's correlation, measures of N_2O emission vs. pH ($CaCl_2$ or H_2O), $p > 0.05$), but did map to differences in 16S community composition across axis 1 in NMDS plots (Table 1, Spearman's correlation NMDS axis 1, Figure 2A). However, significant correlation to the full dissimilarity matrix based on Mantel tests (Table 1) was not achieved unless all distance specific replications were included in analyses (Figure S3). Similar trends were observed for alternative emission potential metrics (Table 1). pH and long-term average daily rainfall were identified as potential drivers of differences in microbial community composition. Both were significantly correlated to overall changes in the dissimilarity matrix, and mapped primarily to NMDS axis 1 and 2 respectively (Table 1, Figure 2B)

We also measured *nosZII* gene copy numbers as a community related functional metric as it has been suggested *nosZII* carrying organisms are important for soil N_2O reduction activity. *nosZII* copy number expressed in various forms (numbers per ng soil DNA, per gram of soil, normalized to 16S copy numbers and relative to *nosZI* copy numbers) were not significantly correlated to N_2O hypothetically emitted % or other

measures of emission potential ($p>0.05$, Spearman's correlation). *nosZII* copy numbers were most strongly correlated with soil pH $CaCl_2$ (Spearman's correlation, $\rho=0.60$, $p<0.01$) and interestingly, were ~10 fold higher in abundance than *nosZI* (Figure 2C).

3.3 Rainfall

In addition to community associations, we assessed the direct relationship between rainfall and soil phenotypes/N_2O emission potential. More concurrent N_2O production/reduction was associated with higher long-term average daily rainfall (Figure 3A). The strength of the correlation was best (and highly significant; $p<0.01$) when rainfall regime was averaged over a prior year or decade, and was not significant when averaged over shorter time span (Table S3). Linear regression of rainfall (10 years) and hypothetically emitted N_2O (%) poorly recapitulated the trends observed in non-parametric and non-continuous analyses (Figure 3B), probably due to the high variability in average daily rainfall among low N_2O emitting soils. Correlations between all rainfall and N_2O emission potential metrics are found in Table S3. Multiple linear regression indicated drainage class and potential evapotranspiration did not aid prediction of N_2O hypothetically emitted (%) with only rainfall producing a significant parameter effect ($p = 0.03$, Table S4).

3.4 Nitrate + nitrite

Final cumulated N_2 levels per vial were inconsistent between soils suggesting significant variation in $NO_3^- + NO_2^-$ concentrations upon initiation of the anoxic incubation period (Figure 4A). Further, comparison of measured soil $NO_3^- + NO_2^-$ before incubation and at the start of the anoxic incubation estimated from cumulative denitrified N (Figure 4A) suggested NO_3^- or NO_2^- was accumulated during the oxic incubation period, presumably due to nitrification of added ammonium. We investigated the potential impact of these variable initial $NO_3^- + NO_2^-$ concentrations as it has previously been demonstrated that N_2O reduction activity is sensitive to NO_3^- and NO_2^- concentration. Predicted $NO_3^- +$

433 NO_2^- porewater concentrations at the start of the anoxic period were not significantly
434 correlated to N_2O hypothetically emitted %, however, significant positive correlations were
435 observed for some alternative measures of N_2O emission potential (Table 2).

436 Normalized N_2 production rates (% of maximum) were plotted against residual NO_3^-
437 + NO_2^- concentrations estimated from denitrification progress at different stages during the
438 anoxic incubation to allow comparison of soil N_2O reduction rates at similar NO_3^- + NO_2^-
439 concentrations (Figure 4B, C). Concurrent soils showed greater % N_2 production rate at
440 greater NO_3^- + NO_2^- levels while most sequential phenotype soils maintained near zero N_2
441 production rates until NO_3^- + NO_2^- fell below 20-10µmol (Figure 4C). However, it should
442 not necessarily be concluded that different sensitivities of N_2O reduction to NO_3^- + NO_2^-
443 explain the variation in soil N_2O reduction/production phenotype, due to confounding by
444 time, N denitrified, the natural progression of denitrification and other unknown factors.
445 Sensitivity of N_2O reduction to NO_3^- + NO_2^- has previously been explained by pH,
446 therefore we overlayed pH onto plots but did not find an explanatory pattern (Figure S4).

447 **3.5 Carbon supplementation**

448 We hypothesized that differences in apparent denitrification phenotypes resulted from
449 electron competition under carbon-limited conditions between earlier steps of
450 denitrification and N_2O reduction. In further incubations, soils representing a range of
451 phenotypes/N_2O emission potentials were amended with both glutamate (to relieve
452 potential carbon limitation) and NH_4NO_3 (to provide NO_3^- for denitrification) or control
453 vials with NH_4NO_3 alone. In most cases, carbon negative controls (Figure 5, left panel)
454 recapitulated the general phenotypic trends observed in initial incubations (Figure 1) but
455 there were some large observable differences, possibly caused by changes to the incubation
456 preparation methodology (omitted oxic preincubation, increased added NH_4NO_3 to 4mM).
457 In particular, soil 40-Fairlie-Geraldine (Figure 5A, top-left) showed a “weakened”

concurrent phenotype, compared with original incubations (N_2O hypothetically emitted %, 0.41 in original vs. 0.80 in second incubation). Differences for other soils were much less dramatic (Table 3). All +N treatments also had higher CO_2 production rates and denitrification process rates, on average 1.44 (average CO_2 production rate) and 1.38 (max N_2O production rate) times higher respectively, compared with original incubations. This may suggest changes made to incubation methodology resulted in higher respiration and probably more available soil carbon.

Carbon amendment had variable impacts on denitrification phenotype, respiration and denitrification rates depending on the soil (Figure 5, Table 3). Added carbon clearly relieved some limitation as we observed increased CO_2 production (Table 3) and reduced time to complete denitrification in all soils (Figure 5), but impacts on denitrification phenotype were not in line with our original hypothesis. Carbon amendments drove concurrent soils (40-Fairlie-Geraldine, 20-Waitaha Valley) towards a more sequential phenotype (increased N_2O hypothetically emitted % and max NO accumulation compared with +N controls, Table 3) while sequential soils (1-Woodend, 33-Rae's Junction) maintained their sequential phenotype (similar N_2O hypothetically emitted % and max NO accumulation compared with +N controls, Table 3). Our C amended intermediate soil 5-Waipapa did not appear to respond in the same way as other soils. The soil accumulated less NO than the N amended control (Difference max NO, 3.26µmol) and showed a variable response in measures of N_2O emission potential (Table 3).

Discussion

The initial incubation experiment unexpectedly revealed a continuum of soil denitrification phenotypes based on the timing of N_2O reduction/production. The most striking soils (Figure 1C) carried out N_2O production and reduction steps almost entirely sequentially, accumulating most N as N_2O in vial headspace before initiating rapid N_2O reduction. In an open vial or pasture soil, this emission pattern is predicted to result in up to 100% emission of produced N_2O, depending on soil physical properties (e.g. depth, water filled porosity) determining the ability of delayed N_2O reduction to transform N_2O before emission. In addition to our initial aim of re-assessing previously observed links between $N_2O/(N_2O+N_2)$, pH and microbial community composition (Samad *et al.*, 2016b, 2016a), we explored the potential causes of these contrasting N_2O production/reduction phenotypes which are hypothesized to be due to a transient mechanism of action, potentially a reversible inhibition or regulatory process.

4.1 The role of pH

The correlation between low pH and high $N_2O/(N_2O+N_2)$ ratio is well documented and has been demonstrated in a variety of experimental systems (Bergaust *et al.*, 2010; Liu *et al.*, 2014; Samad *et al.*, 2016a). As such, we were surprised to find that pH was not correlated to measures of N_2O emission potential in the present study. It is possible that variability of other factors influencing N_2O emission ratios overshadowed a pH effect in this particular data. pH correlations with $N_2O/(N_2O+N_2)$ ratios are most often observed through variable pH manipulation within a single site or soil e.g. (Čuhel *et al.*, 2010; Liu *et al.*, 2010; Simek and Cooper, 2002), while the studied soils were from varying geographical locations with variable management.

Alternatively, unobserved pH changes before the anoxic incubation period could obscure a true correlation. Comparisons between measured soil NO_3^- + NO_2^- before oxic incubation and predicted NO_3^- + NO_2^- at the beginning of the anoxic period (based on final N_2 accumulated) showed nitrification must have occurred in most soils while they were under oxic conditions (Figure 4A). Nitrification of ammonium results in the release of two H^+ ions per molecule of ammonium oxidized (Rowell and Wild, 1985; Zhao *et al.*, 2014) and therefore could have caused significant acidification of incubated soils in the present study, making initial pH measurements irrelevant. Various lines of evidence seem to counter this hypothesis:

1. There was no correlation between nitrification activity, predicted from the difference in initial measured NO_3^- + NO_2^- vs. estimated at the start of the anoxic incubation and $N_2O/(N_2O+N_2)$ suggesting that pH changes due to nitrification were negligible or at least too minor to completely define soil pH trends (Spearmans's correlation $N_2O/(N_2O+N_2)$ vs. NO_3^- + NO_2^- accumulation during oxic incubation µmol, $\rho=0.15$, $p > 0.05$).

2. Samad *et al.* (2016b, 2016a) observed a significant correlation between initial soil pH and $N_2O/(N_2O+N_2)$ using the same incubation methodology used here. Therefore, variable acidification was not an issue, even though high gaseous N accumulation suggested substantial nitrification occurred.

3. pH was still not correlated to $N_2O/(N_2O+N_2)$ in repeated soil incubations without an oxic period (and presumably minimal nitrification) (Spearmans's correlation, $\rho=0.10$, $p > 0.05$).

4. Omission of the oxic incubation period usually resulted in increased hypothetically emitted N_2O (%) compared with initial incubations (Table 3). The opposite would be expected if significant amounts of acidification occurred during oxic periods.

Based on these arguments, we tentatively conclude that factors other than pH were the most important drivers of N_2O production/reduction phenotypes and $N_2O/(N_2O+N_2)$ in the current study but do not doubt that soil pH could exert effects on the observed phenotype, associated $N_2O/(N_2O+N_2)$ ratios and NO accumulation patterns based on retrospective analysis of (Samad *et al.*, 2016b, 2016a). Previous evidence suggests pH based control of $N_2O/(N_2O+N_2)$ is due to a post-trasnscriptional impairment of enzyme maturation in the periplasm (Bergaust *et al.*, 2010; Liu *et al.*, 2014), however, we suggest this does not explain well the delayed nature of N_2O reduction observed in (Samad *et al.*, 2016a) or elsewhere (Liu *et al.*, 2010).

4.2 The role of microbial community composition and distal regulators in determining observed phenotypes

Samad *et al.* (2016b, 2016a) previously linked $N_2O/(N_2O+N_2)$, pH, and 16S microbial community composition using the same methodology used here. However, it remained unclear whether correlations between $N_2O/(N_2O+N_2)$ and 16S microbial community composition indicated a true causal link. Based on the well-known impacts of pH on both $N_2O/(N_2O+N_2)$ (Simek and Cooper, 2002) and microbial community structuring (Lauber *et al.*, 2009; Kaminsky *et al.*, 2017; Samad *et al.*, 2016b), a plausible explanation was that pH independently determined $N_2O/(N_2O+N_2)$ and microbial community composition. A similar 3-way correlation emerged here but with average daily rainfall at the sample sites in place of pH. Again, it is plausible that long term rainfall patterns or a linked variable separately influenced $N_2O/(N_2O+N_2)$ and community composition, however, taken together Samad *et al.* (2016a, 2016b) and the present study may indicate an alternate story: a consistent link

(though less strong here than Samad *et al.* (2016a)) between N_2O emission potential and community composition and a consistent continuum of N_2O production/reduction phenotypes (though less obvious in (Samad *et al.*, 2016a)) both occurring across different soil sets among alternate potential confounding drivers (rainfall patterns here, pH in (Samad *et al.*, 2016b). Thus, there is some increased support for a true link between 16S community composition and N_2O emission potential. Soil phenotypes were clearly sensitive to manipulations i.e. carbon addition (Figure 5 Left side vs. right side) and methodology changes altered N_2O emission potential/phenotypes (Figure 1 vs. Figure 5), but different communities could hypothetically display a greater propensity for more sequential or concurrent denitrification under consistent proximal regulators. This could be due to, for example, alternate denitrification regulatory phenotypes (e.g. early *nosZ* expression) of community members between soils (Liu *et al.*, 2013; Lycus *et al.*, 2017; Bergaust *et al.*, 2011).

It remains unclear how exactly rainfall patterns shape the denitrifying community and N_2O emission potential, though past hydrological experience has previously been linked to the timing of soil N_2O reduction (Zhu *et al.*, 2013). Short term rainfalls prior to sampling, soil storage moisture and soil moisture content at the time of experimentation were irrelevant to N_2O emission potential, therefore a longterm effect on chemistry or community selection is implied. Selection could involve recruitment of successful organisms from the available biosphere and, over longer periods, evolutionary adaption e.g. (Lynch and Neufeld, 2015; Parkin *et al.*, 1985). We hypothesize long periods of soil saturation, ensuing anoxia and slowed diffusion of N_2O provide a niche in which complete and concurrent denitrifiers are more successful. Under more transient and less complete anoxia (low rainfall), denitrifiers showing short term prioritization of $NO_3^- + NO_2^-$ may be selected due to a greater energy yield of $NO_3^- + NO_2^-$ (Giles *et al.*, 2012; Simon and Klotz, 2013), their immediacy in the denitrification pathway, a higher availability of nitrate from

574 nitrification coupled denitrification (due to semi-oxic conditions) (Wrage *et al.*, 2001), or
575 the relatively poor (in comparison to prior reductases) activity of N_2O reductase in the
576 presence of O_2 (Morley *et al.*, 2008).

577 The abundance and diversity of Clade II nitrous oxide reductase genes is previously
578 predicted to control the N_2O sink capacity of soils (Jones *et al.*, 2014) as nosZII carrying
579 denitrifiers are more likely to lack N_2O producing steps (Graf *et al.*, 2014). Although
580 *nosZII* gene abundances and *nosZI/nosZII* gene abundance ratios here were related to pH
581 differences (Spearman correlation $N_2O/(N_2O+N_2)$ vs. *nosZI/nosZII* ρ=-0.47, $p < 0.05$, vs.
582 n*osZII* copy numbers ρ=-0.60, $p < 0.05$), as in previous studies (Jones *et al.*, 2014; Samad
583 *et al.*, 2016b), they did not show any correlation to $N_2O/(N_2O+N_2)$ product ratios
584 (Spearman's correlation, $p > 0.05$) in this study, suggesting that they probably did not
585 determine N_2O sink capacity. Indeed, the decoupling of $N_2O/(N_2O+N_2)$ product ratios and
586 *nosZII* abundances/ratios in this study under circumstances where pH was not found to
587 drive $N_2O/(N_2O+N_2)$ product ratios may weaken prior claims (Jones *et al.*, 2014; Samad *et*
588 *al.*, 2016b) that *nosZII* abundances affected $N_2O/(N_2O+N_2)$ product ratios rather than
589 simply varying with the shared driver of pH.

590 Higher N_2O emission potential for sequential soils occurred due to poor timing of
591 N_2O reduction rather than a deficit in actual N_2O reduction capability (Figure 1), therefore
592 a genotype based explanation (lack of *nosZ* containing denitrifiers vs. high presence of non-
593 denitrifying nitrous oxide reducers only containing *nosZ*) for the differing N_2O
594 production/reduction phenotypes seems unlikely. Some of the lowest nosZII gene copy
595 numbers were actually seen in concurrent soils with lower N_2O emission potential (Figure
596 2C, e.g. 39-Lake Heron, 40-Fairlie-Geraldine, 27-Lumsden). Quantification of *nosZ*
597 transcripts may have been more informative in the current study as it remains unclear
598 whether *nosZ* expression was just delayed in sequential N_2O producing/reducing soils or

599 early function was impaired by post-transcriptional effects, which are previously observed
600 to occlude transcription based effects (e.g. Liu *et al.*, 2010, 2014).

601 **4.3 The role of proximal regulators in determining observed phenotypes**

602 **4.3.1 The effect of carbon availability**

603 Enhanced N_2O accumulation in response to carbon limitation has been attributed to
604 competition for electrons between the different denitrification enzymes (Pan *et al.*, 2013;
605 Ribera-Guardia *et al.*, 2014; Dendooven *et al.*, 1994). Here, carbon additions were made to
606 denitrifying soil incubations to test the hypothesis that sequential phenotype soils have
607 limited electron supply and thus direct electrons preferentially towards the earlier steps of
608 denitrification. This mechanism would also explain why impaired N_2O reduction activity
609 was transient i.e. as prior electron acceptors deplete, competition would be relieved. Under
610 these circumstances, addition of carbon should lead to increased electron availability (as
611 long as regeneration of the electron carrier pool was not already maximal) and presumably
612 increased early N_2O reduction. Experimental evidence here mostly contradicted that
613 hypothesis. Carbon addition to the hypothesized "electron limited" sequential soils did not
614 result in a consistent shift towards a concurrent phenotype, though increases in
615 denitrification process rates do suggest that those soils were indeed somewhat carbon
616 limited (Table 3). The overall trend observed was that carbon availability, substrate
617 type/quality, C/N ratios or some other related effect sustained or drove soils toward a
618 sequential phenotype with increased N_2O hypothetically emitted % and NO accumulation,
619 excepting soil 20-Waitaha (Figure 5). A possible explanation is that carbon addition
620 preferentially stimulated NO_3^- + NO_2^- reduction leading to accumulation of NO which may
621 in turn have an inhibitory impact on N_2O reductase (see 4.3.2). Though it remains unclear
622 why the initial denitrification steps would be preferentially enhanced.

623 Comparisons to initial soil incubations may also be informative about the role of
624 carbon, though differences in methodology and initial NO_3^- concentrations should be taken
625 into consideration. These initial soil incubations probably had less carbon available for
626 denitrification due carbon consumption during oxic pre-incubations as evidenced by lower
627 CO_2 production rates during denitrification (Table 3). If the crude assumption is made that
628 average CO_2 production during denitrification was proportional to carbon availability then
629 hypothetical N_2O emission potential in many of these soils (40-Fairlie-Geraldine, 20-
630 Waitaha Valley, 1-Woodend) appear to exhibit a positive correlation to carbon availability
631 (Table 3).

632 Based on the above observations it seems plausible that differences in carbon
633 accounted for some of the phenotypic variation observed between soils in the original
634 incubations. Direct measurement of starting carbon concentrations (e.g. total C, dissolved
635 organic C) or substrates by mass spectrometry in soils would be beneficial in future
636 investigations of the observed denitrification phenotypes.

637 **4.3.2 Nitric oxide accumulation, nitrite accumulation and nitrate concentration**

638 Accumulation of prior N oxyanions/oxides (NO_3^-, NO_2^-, NO) can impair N_2O
639 reduction activity (Blackmer and Bremner, 1978; Firestone *et al.*, 1979; Gaskell *et al.*,
640 1981; Senbayram *et al.*, 2012; Ha *et al.*, 2015; Pan *et al.*, 2013; Zhou *et al.*, 2008; Frunzke
641 and Zumft, 1986) due to N reductase competition for electrons e.g. (Pan *et al.*, 2013;
642 Dendooven *et al.*, 1994) or alternate mechanisms such as direct inhibitory interaction
643 between NO and N_2O reductase (Frunzke and Zumft, 1986), NO_2^- protonation to inhibitory
644 nitrous acid (Zhou *et al.*, 2008) or NO_2^- based enhancement of obligate N_2O endproduct
645 producing fungi (Maeda *et al.*, 2015). Again, transient accumulation of N oxyanions/oxides
646 is in line with transient impairment of N_2O reductase in sequential N_2O producing/reducing
647 soils. The NO accumulation patterns and timing are particularly conspicuous: NO

accumulation was higher in sequential N_2O producing/reducing soils (Spearman's correlation, average μmol NO $vial^{-1}$ vs. N_2O hypothetically emitted %, $\rho=0.80$, $p<0.0001$), increased N_2O reduction coincided with rapid depletion of NO (Figure 1C), concurrent N_2O producing/reducing soils eventually stabilized NO levels to a low steady state (Figure 1A), and C amendments increasing or decreasing N_2O hypothetically emitted % also increased/decreased max NO accumulation (Table 3). Based on these observations we hypothesize that sequential type soils were unable to maintain NO concentrations below an inhibitory level, resulting in impaired N_2O reduction until NO production ceased. Alternatively, NO accumulation may be indicative of a significant NO_2^- pool stimulating NO production by both abiotic and biotic processes (Lim *et al.*, 2018). NO_2^- reductase is proposed to be particularly competitive with N_2O reductase for electrons due to a shared use of the electron carrier cytochrome C550 (Richardson *et al.*, 2009; Pan *et al.*, 2013), therefore, tracking of endogenous NO_2^- and evaluating responses to exogenous NO_2^- in future experimentation is highly desirable.

Correlations between some measures of N_2O emission potential and predicted $NO_3^- + NO_2^-$ at the start of anoxia (Table 2) suggest initial N supply may have impacted the observed gas kinetic patterns. However, we are skeptical based on a lack of correlation with the most pertinent variables (N_2O hypothetically emitted % and $N_2O/(N_2O+N_2)$ (max N_2O)) and potential biases in the other measures. For instance, measures taken at the 50hr anoxia timepoint will capture higher ratios in soils with high $NO_3^- + NO_2^-$ because they typically take longer to denitrify. Further, soils showed diverse relative N_2O reduction rates at the same level of remaining $NO_3^- + NO_2^-$ (Figure 4B, C).

$NO_3^- + NO_2^-$ concentration effects could hypothetically be occluded in correlations between separate soils if individual soils had dramatically differing sensitivities to the similar NO_3^- or NO_2^- concentrations. Differing sensitivity of N_2O reduction to $NO_3^- + NO_2^-$

concentration in different soils has been previously reported, with higher sensitivity in lower pH soils (Blackmer and Bremner, 1978; Firestone *et al.*, 1979; Gaskell *et al.*, 1981). However, we did not observe pH based ranking of soils once NO_3^- + NO_2^- availability was accounted for (Figure S4), and this analysis cannot be considered conclusive due to the potential bias of denitrification progress; because of differences in initial NO_3^-+NO_2^-, different soils reached the same remaining NO_3^- + NO_2^- at different times and different amounts of NO_3^- + NO_2^- were already utilized. Experiments applying varying concentrations of NO_3^- or NO_2^- to pH manipulated soils or using temporally constant NO_3^- concentrations (chemostats) would be necessary to understand the true impact of NO_3^- and NO_2^- on the observed denitrification phenotypes and N_2O emission potential.

4.4 Conclusion

Here, we demonstrate considerable variation in N_2O emission potential for New Zealand pasture soils based on the timing and activity of N_2O reduction and associated with the accumulation of NO gas. We show an association between N_2O production/reduction phenotypes and microbial communities in the absence of a pH effect and in conjunction with results from Samad *et al.* (2016b, 2016a) suggest this improves the plausibility of a true link between community composition and the observed phenotypes/N_2O emission potential. Additional correlates of N_2O emission potential/emission phenotypes are identified at both distal (long term rainfall) and proximal levels (carbon availability) which may be linked by a common mechanism of NO accumulation and inhibition. Further research on the phenomena described here should focus on directly testing the impact of NO concentrations on the observed phenotypes, the potential accumulation of NO_2^- in sequential type soils, and the potential for regulatory effects such as delayed transcription of *nosZ*.

Acknowledgements

This work was funded by the New Zealand Government through the New Zealand Fund for Global Partnerships in Livestock Emissions Research to support the objectives of the Livestock Research Group of the Global Research Alliance on Agricultural Greenhouse Gases (Agreement number: 16084 and SOW12-GPLER-OU-SM) awarded to SEM and the University of Otago, New Zealand. MH was funded by a University of Otago Postgraduate Scholarship. PD P received funding from the FACCE-ERA-GAS project MAGGE-pH under the grant agreement no. 696356. We would like to thank the Nitrogen group at the Norwegian University of Life Sciences NMBU for access to lab, robotic autosamplers, experimental and technical assistance. We also thank Steve Wakelin and AgResearch for providing historic physicochemical data and preliminary DNA samples for the analysed soils.

References

2º Institute. (2016). Global N_2O Levels. https://www.n2olevels.org/ (Accessed July 12, 2019).

Altschul SF, Gish W, Miller W, Myers EW, Lipman DJ. (1990). Basic local alignment search tool. *J Mol Biol* **215**: 403–410.

ASTM D2216-10. (2010). Standard Test Methods for Laboratory Determination of Water (Moisture) Content of Soil and Rock by Mass. *ASTM Int*. e-pub ahead of print, doi: 10.1520/D2216-10.N.

Baggs EM. (2011). Soil microbial sources of nitrous oxide: recent advances in knowledge, emerging challenges and future direction. *Curr Opin Environ Sustain* **3**: 321–327.

Bakken LR, Frostegård Å, Dörsch P, Almøy T. (2015). A critique of Jones et al NCC 2014. *Researchgate*.

Bergaust L, Bakken LR, Frostegård A. (2011). Denitrification regulatory phenotype, a new term for the characterization of denitrifying bacteria. *Biochem Soc Trans* **39**: 207–212.

Bergaust L, Mao Y, Bakken LR, Frostegard A. (2010). Denitrification Response Patterns during the Transition to Anoxic Respiration and Posttranscriptional Effects of Suboptimal pH on Nitrogen Oxide Reductase in Paracoccus denitrificans. *Appl Environ Microbiol* **76**: 6387–6396.

Blackmer AM, Bremner JM. (1978). Inhibitory effect of nitrate on reduction of N_2O to N_2

726 by soil microorganisms. *Soil Biol Biochem* **10**: 187–191.

727 Braman RS, Hendrix SA. (1989). Nanogram nitrite and nitrate determination in
728 environmental and biological materials by vanadium (III) reduction with
729 chemiluminescence detection. *Anal Chem* **61**: 2715–2718.

730 Bremner JM. (1997). Sources of nitrous oxide in soils. *Nutr Cycl Agroecosystems* **49**: 7–16.

731 Caporaso JG, Kuczynski J, Stombaugh J, Bittinger K, Bushman FD, Costello EK, *et al.*
732 (2010). QIIME allows analysis of high-throughput community sequencing data. *Nat*
733 *Methods* **7**: 335–336.

734 Caporaso JG, Lauber CL, Walters WA, Berg-Lyons D, Huntley J, Fierer N, *et al.* (2012).
735 Ultra-high-throughput microbial community analysis on the Illumina HiSeq and MiSeq
736 platforms. *ISME J* **6**: 1621–1624.

737 Cichota R, Snow VO, Tait AB. (2008). A functional evaluation of virtual climate station
738 rainfall data. *New Zeal J Agric Res* **51**: 317–329.

739 Čuhel J, Šimek M, Laughlin RJ, Bru D, Chèneby D, Watson CJ, *et al.* (2010). nsights into
740 the effect of soil pH on N_2O and N_2 emissions and denitrifier community size and activity.
741 *Appl Environ Microbiol* **76**: 1870–1878.

742 Davidson EA. (2009). The contribution of manure and fertilizer nitrogen to atmospheric
743 nitrous oxide since 1860. *Nat Geosci* **2**: 659–662.

744 Dendooven L, Splatt P, Anderson JM, Scholefield D. (1994). Kinetics of the denitrification

745 process in a soil under permanent pasture. *Soil Biol Biochem* **26**: 361–370.

746 Dixon P. (2003). VEGAN, a package of R functions for community ecology. *J Veg Sci* **14**:
747 927–930.

748 Domeignoz-Horta LA, Spor A, Bru D, Breuil M-C, Bizouard F, Léonard J, *et al.* (2015).
749 The diversity of the N_2O reducers matters for the N_2O:N_2 denitrification end-product ratio
750 across an annual and a perennial cropping system. *Front Microbiol* **6**: 971.

751 Edgar RC. (2010). Search and clustering orders of magnitude faster than BLAST.
752 *Bioinformatics* **26**: 2460–2461.

753 Firestone MK, Smith MS, Firestone RB, Tiedje JM. (1979). The influence of nitrate, nitrite,
754 and oxygen on the composition of the gaseous products of denitrification in soil. *Soil Sci*
755 *Soc Am J* **43**: 1140.

756 Frunzke K, Zumft WG. (1986). Inhibition of nitrous-oxide respiration by nitric oxide in the
757 denitrifying bacterium Pseudomonas perfectomarina. *BBA - Bioenerg* **852**: 119–125.

758 Gaskell JF, Blackmer AM, Bremner JM. (1981). Comparison of effects of nitrate, nitrite,
759 and nitric oxide on reduction of nitrous oxide to dinitrogen by soil microorganisms. *Soil Sci*
760 *Soc Am J* **45**: 1124.

761 Giles M, Morley N, Baggs EM, Daniell TJ. (2012). Soil nitrate reducing processes –
762 drivers, mechanisms for spatial variation, and significance for nitrous oxide production.
763 *Front Microbiol* **3**: 1–16.

764 Gillam KM, Zebarth BJ, Burton DL. (2008). Nitrous oxide emissions from denitrification
765 and the partitioning of gaseous losses as affected by nitrate and carbon addition and soil
766 aeration. *Can J Soil Sci* **88**: 133–143.

767 Graf DRH, Jones CM, Hallin S. (2014). Intergenomic comparisons highlight modularity of
768 the denitrification pathway and underpin the importance of community structure for N2O
769 emissions De Crécy-Lagard V (ed). *PLoS One* **9**: e114118.

770 Groffman P, Tiedje J, Robertson GP, Christensen S. (1988). Denitrification at different
771 temporal and geographical scales: proximal and distal controls. In: *Advances in Nitrogen*
772 *Cycling in Agricultural Systems*. pp 174–192.

773 Ha TKT, Maeda M, Fujiwara T, Nagare H, Akao S. (2015). Effects of soil type and nitrate
774 concentration on denitrification products (N_2O and N_2) under flooded conditions in
775 laboratory microcosms. *Soil Sci Plant Nutr* **61**: 999–1004.

776 Halvorson H. (1972). Utilization of single L-amino acids as sole source of carbon and
777 nitrogen by bacteria. *Can J Microbiol* **18**: 1647–1650.

778 Hartman AL, Lough DM, Barupal DK, Fiehn O, Fishbein T, Zasloff M, *et al.* (2009).
779 Human gut microbiome adopts an alternative state following small bowel transplantation.
780 *Proc Natl Acad Sci* **106**: 17187–17192.

781 Henry S, Bru D, Stres B, Hallet S, Philippot L. (2006). Quantitative detection of the nosZ
782 gene, encoding nitrous oxide reductase, and comparison of the abundances of 16S rRNA,
783 narG, nirK, and nosZ genes in soils. *Appl Environ Microbiol* **72**: 5181–5189.

784 Intergovernmental Panel on Climate Change. (2013). Climate change 2013 the physical
785 science basis: Working Group I contribution to the fifth assessment report of the
786 intergovernmental panel on climate change. Cambridge University Press: Cambridge.

787 Jones CM, Graf DRH, Bru D, Philippot L, Hallin S. (2013). The unaccounted yet abundant
788 nitrous oxide-reducing microbial community: a potential nitrous oxide sink. *ISME J* **7**:
789 417–26.

790 Jones CM, Spor A, Brennan FP, Breuil M-C, Bru D, Lemanceau P, *et al.* (2014). Recently
791 identified microbial guild mediates soil N_2O sink capacity. *Nat Clim Chang* **4**: 801–805.

792 Kaminsky R, Trouche B, Morales SE. (2017). Soil classification predicts differences in
793 prokaryotic communities across a range of geographically distant soils once pH is
794 accounted for. *Sci Rep* **7**: 45369.

795 Lauber CL, Hamady M, Knight R, Fierer N. (2009). Pyrosequencing-based assessment of
796 soil pH as a predictor of soil bacterial community structure at the continental scale. *Appl*
797 *Environ Microbiol* **75**: 5111–5120.

798 Lauber CL, Strickland MS, Bradford MA, Fierer N. (2008). The influence of soil properties
799 on the structure of bacterial and fungal communities across land-use types. *Soil Biol*
800 *Biochem* **40**: 2407–2415.

801 Lim NYN, Frostegård Å, Bakken LR. (2018). Nitrite kinetics during anoxia: The role of
802 abiotic reactions versus microbial reduction. *Soil Biol Biochem* **119**: 203–209.

803 Liu B, Frostegård Å, Bakken LR. (2014). Impaired reduction of N_2O to N_2 in acid soils is

804 due to a posttranscriptional interference with the expression of nosZ Bailey M (ed). *MBio*
805 **5**: e01383-14.

806 Liu B, Mao Y, Bergaust L, Bakken LR, Frostegård Å. (2013). Strains in the genus Thauera
807 exhibit remarkably different denitrification regulatory phenotypes. *Environ Microbiol* **15**:
808 2816–2828.

809 Liu B, Mørkved PT, Frostegård Å, Bakken LR. (2010). Denitrification gene pools,
810 transcription and kinetics of NO, N_2O and N_2 production as affected by soil pH. *FEMS*
811 *Microbiol Ecol* **72**: 407–417.

812 LRIS. (2020). New Zealand Fundamental Soil Layer. https://lris.scinfo.org.nz/ (Accessed
813 July 1, 2020).

814 Lycus P, Bøthun KL, Bergaust L, Shapleigh JP, Bakken LR, Frostegård Å. (2017).
815 Phenotypic and genotypic richness of denitrifiers revealed by a novel isolation strategy.
816 *ISME J* **11**: 2219–2232.

817 Lynch MDJ, Neufeld JD. (2015). Ecology and exploration of the rare biosphere. *Nat Rev*
818 *Microbiol* **13**: 217–229.

819 Maeda K, Spor A, Edel-Hermann V, Heraud C, Breuil MC, Bizouard F, *et al.* (2015). N_2O
820 production, a widespread trait in fungi. *Sci Rep* **5**: 9697.

821 McMurdie PJ, Holmes S. (2013). phyloseq: an R package for reproducible interactive
822 analysis and graphics of microbiome census data. *PLoS One* **8**: e61217.

823 Molstad L, Dörsch P, Bakken LR. (2007). Robotized incubation system for monitoring
824 gases (O_2, NO, N_2O N_2) in denitrifying cultures. *J Microbiol Methods* **71**: 202–211.

825 Morales SE, Jha N, Saggar S. (2014). Biogeography and biophysicochemical traits link
826 N_2O emissions, N_2O emission potential and microbial communities across New Zealand
827 pasture soils. *Soil Biol Biochem* **82**: 87–98.

828 Morley N, Baggs EM, Dörsch P, Bakken L. (2008). Production of NO, N2O and N2 by
829 extracted soil bacteria, regulation by NO2(-) and O2 concentrations. *FEMS Microbiol Ecol*
830 **65**: 102–12.

831 Myhre G, Shindell D, Bréon F, Collins W, Fuglestvedt J, Huang J, *et al.* (2013).
832 Anthropogenic and natural radiative forcing. In: Climate change 2013: the physical science
833 basis. Contribution of working group I. Cambridge University Press: Cambridge.

834 NIWA. (2017). CliFlo: NIWA's National Climate Databasele. http://cliflo.niwa.co.nz/
835 (Accessed May 17, 2017).

836 Oenema O, Wrage N, Velthof GL, van Groenigen JW, Dolfing J, Kuikman PJ. (2005).
837 Trends in global nitrous oxide emissions from animal production systems. *Nutr Cycl*
838 *Agroecosystems* **72**: 51–65.

839 Pan Y, Ni B-J, Bond PL, Ye L, Yuan Z. (2013). Electron competition among nitrogen
840 oxides reduction during methanol-utilizing denitrification in wastewater treatment. *Water*
841 *Res* **47**: 3273–3281.

842 Parkin TB, Sexstone AJ, Tiedje JM. (1985). Adaptation of Denitrifying Populations to Low

Soil pH †. *Appl Environ Microbiol* **49**: 1053–1056.

Qu Z, Wang J, Almøy T, Bakken LR. (2014). Excessive use of nitrogen in Chinese agriculture results in high $N_2O/(N_2O+N_2)$ product ratio of denitrification, primarily due to acidification of the soils. *Glob Chang Biol* **20**: 1685–98.

Quast C, Pruesse E, Yilmaz P, Gerken J, Schweer T, Yarza P, *et al.* (2013). The SILVA ribosomal RNA gene database project: improved data processing and web-based tools. *Nucleic Acids Res* **41**: D590-6.

R Core Team. (2016). R: A language and environment for statistical computing. https://www.r-project.org/.

Ravishankara AR, Daniel JS, Portmann RW. (2009). Nitrous oxide (N_2O): the dominant ozone-depleting substance emitted in the 21st century. *Science* **326**: 123–125.

Ribera-Guardia A, Kassotaki E, Gutierrez O, Pijuan M. (2014). Effect of carbon source and competition for electrons on nitrous oxide reduction in a mixed denitrifying microbial community. *Process Biochem* **49**: 2228–2234.

Richardson D, Felgate H, Watmough N, Thomson A, Baggs E. (2009). Mitigating release of the potent greenhouse gas N_2O from the nitrogen cycle – could enzymic regulation hold the key? *Trends Biotechnol* **27**: 388–397.

Roco CA, Bergaust LL, Bakken LR, Yavitt JB, Shapleigh JP. (2017). Modularity of nitrogen-oxide reducing soil bacteria: linking phenotype to genotype. *Environ Microbiol* **19**: 2507–2519.

863 Rowell DL, Wild A. (1985). Causes of soil acidification: a summary. *Soil Use Manag* **1**:
864 32–33.

865 Samad MS, Bakken LR, Nadeem S, Clough TJ, de Klein CAM, Richards KG, *et al.*
866 (2016a). High-Resolution Denitrification Kinetics in Pasture Soils Link N2O Emissions to
867 pH, and Denitrification to C Mineralization Lehman RM (ed). *PLoS One* **11**: e0151713.

868 Samad MS, Biswas A, Bakken LR, Clough TJ, de Klein CAM, Richards KG, *et al.*
869 (2016b). Phylogenetic and functional potential links pH and N_2O emissions in pasture soils.
870 *Sci Rep* **6**: 35990.

871 Senbayram M, Chen R, Budai A, Bakken L, Dittert K. (2012). N_2O emission and the
872 $N_2O/(N_2O+N_2)$ product ratio of denitrification as controlled by available carbon substrates
873 and nitrate concentrations. *Agric Ecosyst Environ* **147**: 4–12.

874 Simek M, Cooper JE. (2002). The influence of pH on denitrification:Progress towards the
875 understanding of this interaction over the last fifty years. *Eur J Soil Sci* **53**: 345–354.

876 Simon J, Klotz MG. (2013). Diversity and evolution of bioenergetic systems involved in
877 microbial nitrogen compound transformations. *Biochim Biophys Acta* **1827**: 114–135.

878 Syakila A, Kroeze C. (2011). The global nitrous oxide budget revisited. *Greenh Gas Meas*
879 *Manag* **1**: 17–26.

880 Tait A, Turner R, Tait A, Turner R. (2005). Generating multiyear gridded daily rainfall
881 over New Zealand. *J Appl Meteorol* **44**: 1315–1323.

882 Thomson AJ, Giannopoulos G, Pretty J, Baggs EM, Richardson DJ. (2012). Biological
883 sources and sinks of nitrous oxide and strategies to mitigate emissions. *Philos Trans R Soc*
884 *Lond B Biol Sci* **367**: 1157–1168.

885 Wakelin S, van Koten C, O'Callaghan M, Brown M. (2013). Physicochemical properties of
886 50 New Zealand pasture soils: a starting point for assessing and managing soil microbial
887 resources. *New Zeal J Agric Res* **56**: 248–260.

888 Wallenstein MD, Myrold DD, Firestone M, Voytek M. (2006). Environmental controls on
889 denitrifying communities and denitrification rates: insights from molecular methods. *Ecol*
890 *Appl* **16**: 2143–52.

891 Weier KL, Doran JW, Power JF, Walters DT. (1993). Denitrification and the
892 dinitrogen/nitrous oxide ratio as affected by soil water, available carbon, and nitrate. *Soil*
893 *Sci Soc Am J* **57**: 66.

894 Wrage N, Velthof GL, Van Beusichem ML, Oenema O. (2001). Role of nitrifier
895 denitrification in the production of nitrous oxide. *Soil Biol Biochem* **33**: 1723–1732.

896 Zhao X, Wang S, Xing G. (2014). Nitrification, acidification, and nitrogen leaching from
897 subtropical cropland soils as affected by rice straw-based biochar: laboratory incubation
898 and column leaching studies. *J Soils Sediments* **14**: 471–482.

899 Zhou Y, Pijuan M, Zeng RJ, Yuan Z. (2008). Free nitrous acid inhibition on nitrous oxide
900 reduction by a denitrifying-enhanced biological phosphorus removal sludge. *Environ Sci*
901 *Technol* **42**: 8260–8265.

902 Zhu J, Mulder J, Solheimslid SO, Dörsch P. (2013). Functional traits of denitrification in a
903 subtropical forest catchment in China with high atmogenic N deposition. *Soil Biol Biochem*
904 **57**: 577–586.

905 Zumft WG. (1997). Cell biology and molecular basis of denitrification. *Microbiol Mol Biol*
906 *Rev* **61**: 533–616.

907 **Figure Legends**

908 **Figure 1.** N gas kinetics of 20 NZ pasture soils amended with 2mM NH_4NO_3 and incubated
909 in a helium atmosphere. The figure shows the wide variation in timing of N_2O reduction
910 (N_2 production) leading to variable N_2O accumulation. N_2O hypothetically emitted (%)
911 (Table S2) was used to evaluate sequentiality of N_2O production/reduction on a continuous
912 scale (soils ordered top left to bottom right) and define soil phenotypes (concurrent (A),
913 intermediate (B) and sequential (C)) based on discrete arbitrary cutoffs. Circles, squares,
914 triangles represent three replicate vials. Concurrent N_2O production/reduction, is associated
915 with specific NO emission pattern: Lower NO accumulation eventually stabilising at a
916 pseudo steady state. Sequential soils usually accumulate higher max NO. Note that the
917 panels have different scaling of N_2O (Orange), N_2 (Black) and NO (Blue) and values are
918 reported as µmol-N per vial. Scaled version available (Figure S1). Version with CO_2
919 available (Figure S2).

920 **Figure 2.** Microbial community analyses reveal links between 16S community composition
921 and N_2O emission potential/phenotypes (A), average daily rainfall over 10 years and pH
922 (B). qPCR reveals greater abundance of nosZII relative to nosZI (C). NMDS ordination
923 plots (A, B) compare prokaryotic dissimilarities (Bray Curtis) of a single pooled mixed
924 sieved soil sample per site. Full distance specific replications are presented in Figure S3.
925 Stress values for ordinations were 0.14. Correlations between variables and NMDS axes or
926 the Bray Curtis dissimilarity matrix are presented in Table 1.

927 **Figure 3.** Relationship between average daily rainfall (average daily mm rainfall over 10
928 years prior to sampling) and N_2O production/reduction phenotypes (A) or N_2O
929 hypothetically emitted % (B). p-value presented is for difference of medians using

930 Wilcoxon rank sum test with chi-squared approximation. Correlations between all rainfall
931 and N_2O emission potential metrics are presented in **Table S3**.

932 **Figure 4.** Normalized soil N_2 production rates (N_2 rate over max N_2 rate in same soil)
933 increase as available $NO_3^- + NO_2^-$ is depleted in anoxic soil incubations amended with 2mM
934 NH_4NO_3. In most soils, predicted $NO_3^- + NO_2^-$ at beginning of anoxic period is greater than
935 measured $NO_3^- + NO_2^-$ immediately following NO_3^- amendment (A) indicating $NO_3^- + NO_2^-$
936 accumulation, most likely due to nitrification during oxic pre-incubations. Plots (C, D)
937 allow comparison of N_2O reduction activity at similar $NO_3^- + NO_2^-$ concentration for each
938 soil. Ranking of soils across Y-axis could indicate potential variation in soil N_2O reduction
939 sensitivity to $NO_3^- + NO_2^-$ concentration, however this ranking simply describes the
940 aforementioned N_2O production/reduction phenotypes (C) and a potential effect cannot be
941 separated from the natural progression of denitrification or other biases.

942 **Figure 5.** Effect of carbon (10mM Na-glutamate + 4mM NH_4NO_3 by flooding and
943 draining) on soil denitrification kinetics in representative soils ranging in N_2O
944 hypothetically emitted (%)/phenotypes: concurrent (A), sequential (B) and intermediate
945 (C). Triplicate incubations per treatment (dots, squares, triangles) were carried out under
946 anoxia without oxic preincubation. Carbon amended treatments right, C negative controls
947 left. Single leaky reps excluded for 20 +N and 40 +C+N. N_2O (Orange), N_2 (Black) and NO
948 (Blue) are reported as μmol-N per vial. Carbon additions shift kinetics in the tested
949 concurrent soils towards sequential N_2O production/reduction and greater NO accumulation
950 while no dramatic change is observed for the sequential or intermediate soils. Graphs with
951 axes scaled to same maximum available (Figure S5)

952 **Tables**

953 **Table 1.** N_2O emission potential and other variable correlations to community dissimilarity

	NMDS axis 1 co-ords (Spearman's)		NMDS axis 2 co-ords (Spearman's)		Bray curtis dissimilarity matrix (Mantel)	
Variable vs. community composition	**rho (ρ)**	**Sig (p)**	**rho (ρ)**	**Sig (p)**	**r statistic**	**Sig (p)**
N_2O hypothetically emitted (%)	-0.51	0.022*	-0.34	0.137	0.18	0.139
IN_2O (50hrs)	-0.64	0.002*	-0.29	0.215	0.15	0.208
IN_2O (N_2 plateau)	-0.40	0.093	-0.34	0.154	0.24	0.073
$N_2O/(N_2O+N_2)$ (50hrs)	-0.70	0.001*	-0.28	0.232	0.26	0.079
$N_2O/(N_2O+N_2)$(max N_2O)	-0.61	0.004*	-0.26	0.262	0.19	0.134
pH H_2O	-0.32	0.165	0.50	0.025*	0.35	0.005*
pH $CaCl_2$	-0.37	0.110	0.35	0.128	0.32	0.008*
Daily average rainfall (10 years)	0.67	0.001*	0.55	0.012*	0.44	0.009*

954

955 *p<0.05

956 **Table 2.** Correlations between predicted NO_3^- + NO_2^- at the start of anoxia and measures of

957 N_2O emission potential

Variable	Spearman's ρ	Sig (p)
IN_2O (50hrs)	0.70	0.001*
IN_2O (N_2 plateau)	0.53	0.019*
$N_2O/(N_2O+N_2)$ (50hrs)	0.54	0.013*
$N_2O/(N_2O+N_2)$ (max N_2O)	0.30	0.200
N_2O hypothetically emitted (%)	0.09	0.701

958

959 *p<0.05

960

961 **Table 3**. Comparison of gas kinetics features across all incubation treatments for five soils

	Concurrent						Sequential						Intermediate		
	Fairlie-Ger (40)			Waitaha (20)			Rae's Junct (33)			Woodend (1)			Waipapa (5)		
Soil	**1st**	**+N**	**+C+N**	**1st**	**+N**	**+C+N**	**1st**	**+N**	**+C+N**	**1st**	**+N**	**+C+N**	**1st**	**+N**	**+C+N**
Av N_2 rate before peak N_2O (µmol/hr)	0.38	0.36	0.10	0.17	0.14	0.06	0.16	0.08	0.10	0.08	0.18	0.22	0.11	0.26	0.54
Av N_2 rate after peak N_2O (µmol/hr)	0.98	2.20	3.08	0.58	0.52	1.87	1.26	1.57	4.65	2.62	2.77	4.22	0.84	1.30	2.40
Max N_2 rate (µmol/hr)	1.39	2.54	4.26	0.76	0.64	3.84	1.51	2.10	6.89	3.65	3.53	5.01	1.04	1.50	3.14
Max N_2O rate (µmol/hr)	0.91	1.60	2.46	0.71	0.84	1.15	1.25	1.59	2.77	2.24	2.81	2.83	0.79	1.11	1.87
Estimated Av total N turnover rate (µmol NO_2^-, NO, N_2O, N_2 N/hr)	2.78	4.40	5.46	1.42	1.50	3.29	2.73	3.27	6.09	4.44	5.59	6.90	1.77	3.10	4.99
Av CO_2 rate (µmol/hr)	1.15	1.92	2.68	0.90	0.92	1.64	1.34	1.51	2.55	1.99	2.91	3.61	0.74	1.27	2.28
Av NO (µmol)	0.10	0.67	1.15	0.04	0.04	0.56	0.61	0.63	0.62	1.54	0.27	0.23	1.34	1.50	0.51
Max NO (µmol)	0.29	2.21	4.64	0.21	0.27	1.27	0.92	2.31	2.51	4.25	1.53	1.23	3.25	6.06	2.79
N_2OI (N_2 plateau)	0.44	0.61	0.69	0.57	0.58	0.80	0.65	0.65	0.69	0.66	0.63	0.70	0.64	0.53	0.55
$N_2O/(N_2O+N_2)$(max N_2O)	0.59	0.79	0.95	0.71	0.80	0.97	0.87	0.94	0.95	0.96	0.93	0.92	0.84	0.79	0.71
Hypothetically emiited N_2O (%)	0.41	0.80	0.92	0.74	0.83	1.00	0.98	0.99	1.00	0.96	0.90	0.96	0.87	0.70	0.74

962

963

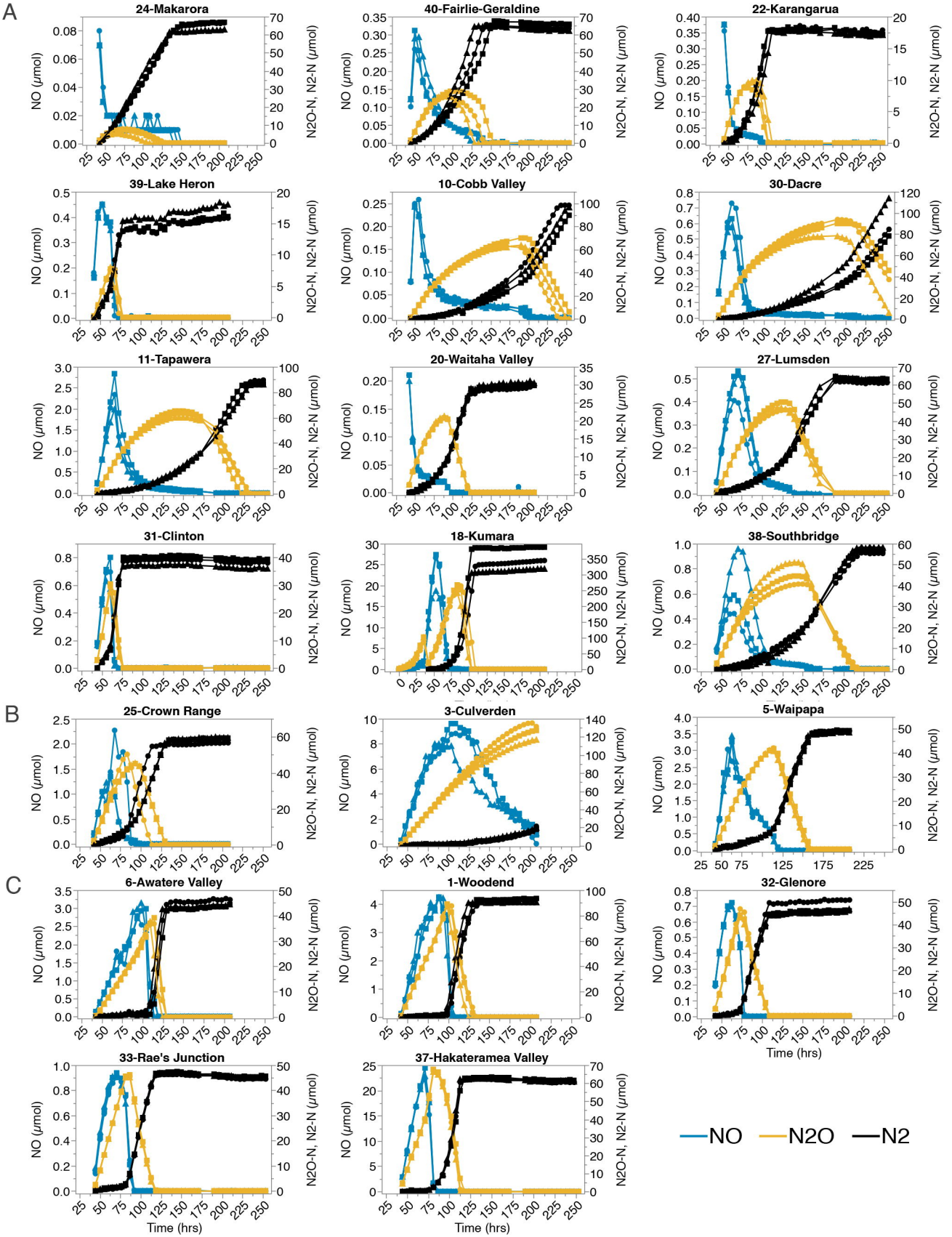
A
24-Makarora
40-Fairlie-Geraldine
22-Karangarua
39-Lake Heron
10-Cobb Valley
30-Dacre
11-Tapawera
20-Waitaha Valley
27-Lumsden
31-Clinton
18-Kumara
38-Southbridge
B
25-Crown Range
3-Culverden
5-Waipapa
C
6-Awatere Valley
1-Woodend
32-Glenore
33-Rae's Junction
37-Hakateramea Valley
NO (µmol)
N2O-N, N2-N (µmol)
Time (hrs)
NO
N2O
N2

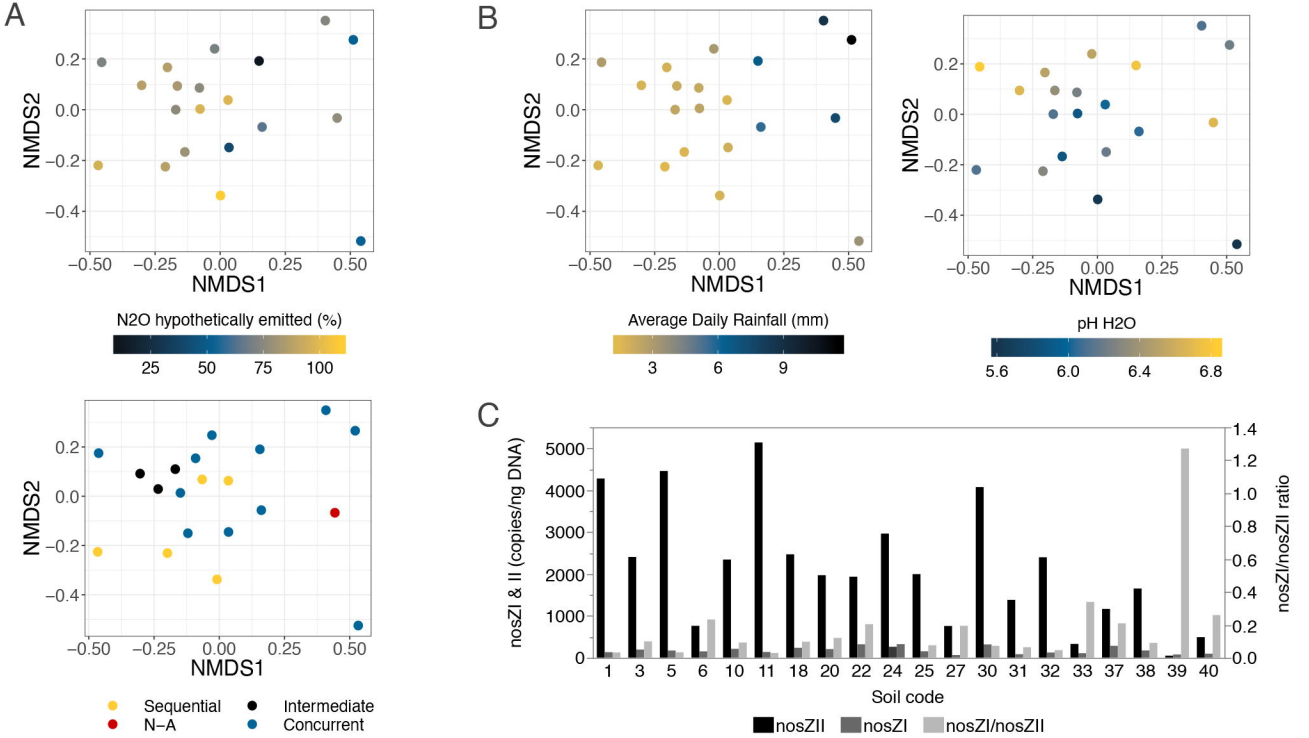
A
NMDS2
NMDS1
N2O hypothetically emitted (%)
25 50 75 100
Sequential
Intermediate
N–A
Concurrent
B
Average Daily Rainfall (mm)
3 6 9
pH H2O
5.6 6.0 6.4 6.8
C
nosZI & II (copies/ng DNA)
nosZI/nosZII ratio
Soil code
1 3 5 6 10 11 18 20 22 24 25 27 30 31 32 33 37 38 39 40
nosZII
nosZI
nosZI/nosZII

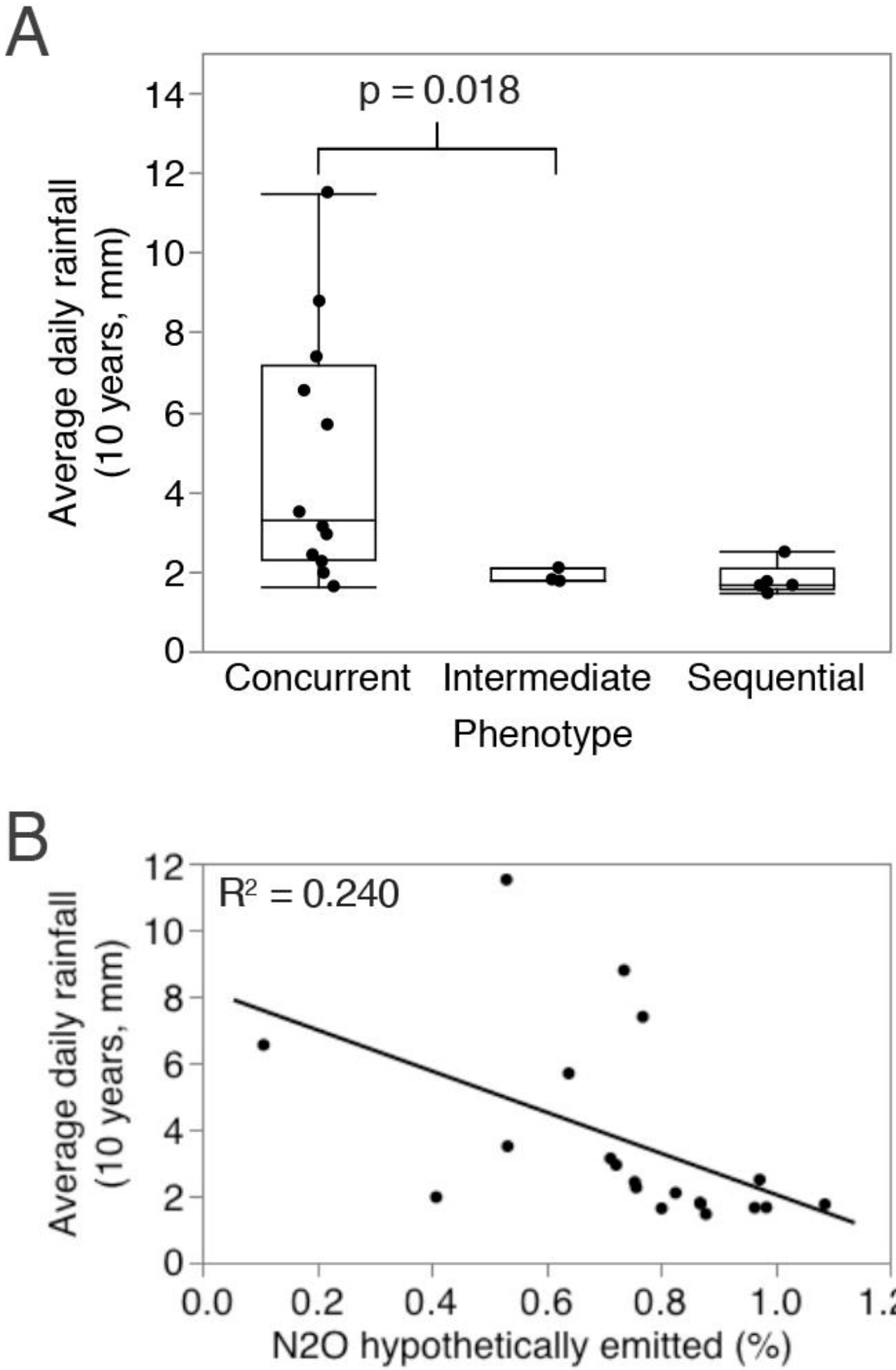
A
p = 0.018
Average daily rainfall
(10 years, mm)
14
12
10
8
6
4
2
0
Concurrent
Intermediate
Sequential
Phenotype
B
R² = 0.240
Average daily rainfall
(10 years, mm)
12
10
8
6
4
2
0
0.0
0.2
0.4
0.6
0.8
1.0
1.2
N2O hypothetically emitted (%)

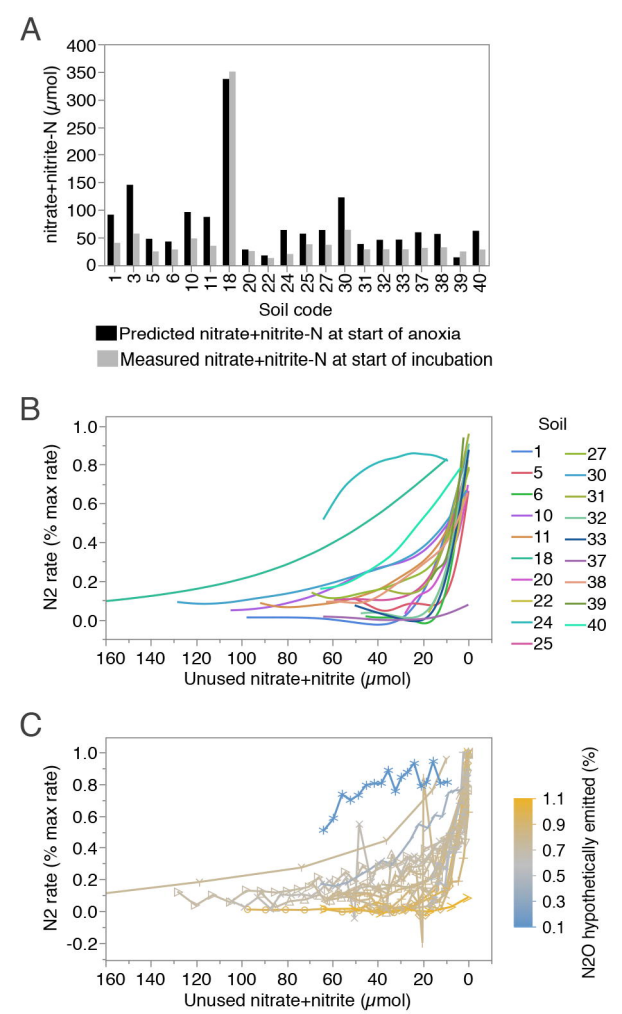
A
nitrate+nitrite-N (μmol)
400
350
300
250
200
150
100
50
0
1 3 5 6 10 11 18 20 22 24 25 27 30 31 32 33 37 38 39 40
Soil code
Predicted nitrate+nitrite-N at start of anoxia
Measured nitrate+nitrite-N at start of incubation
B
N2 rate (% max rate)
1.0
0.8
0.6
0.4
0.2
0.0
160 140 120 100 80 60 40 20 0
Unused nitrate+nitrite (μmol)
Soil
1
5
6
10
11
18
20
22
24
25
27
30
31
32
33
37
38
39
40
C
N2 rate (% max rate)
1.0
0.8
0.6
0.4
0.2
0.0
-0.2
160 140 120 100 80 60 40 20 0
Unused nitrate+nitrite (μmol)
N2O hypothetically emitted (%)
1.1
0.9
0.7
0.5
0.3
0.1

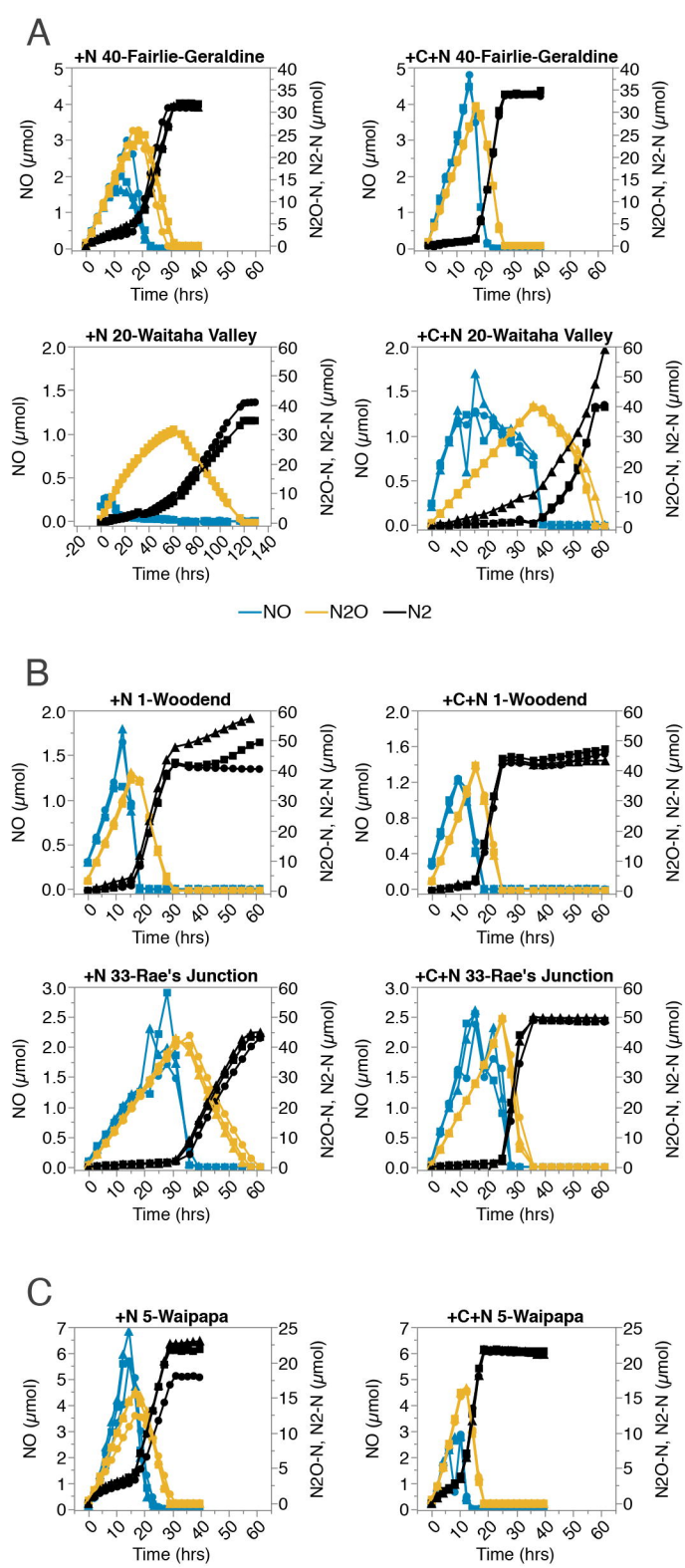
A
+N 40-Fairlie-Geraldine
+C+N 40-Fairlie-Geraldine
+N 20-Waitaha Valley
+C+N 20-Waitaha Valley
NO (µmol)
N2O-N, N2-N (µmol)
Time (hrs)
NO
N2O
N2
B
+N 1-Woodend
+C+N 1-Woodend
+N 33-Rae's Junction
+C+N 33-Rae's Junction
C
+N 5-Waipapa
+C+N 5-Waipapa